

## Optimization of energy-separation filter in multilayer detectors for single-shot dual-energy x-ray imaging

Junwoo Kim<sup>a</sup>, Dong Woon Kim<sup>a</sup>, Ho Kyung Kim<sup>a,b\*</sup>

<sup>a</sup>School of Mechanical Engineering, Pusan National University, Busan 46241, Republic of Korea

<sup>b</sup>Center for Advanced Medical Engineering, Pusan National University, Busan 46241, Republic of Korea

\*Corresponding author: hokyung@pusan.ac.kr

### 1. Introduction

A conventional dual-energy (DE) x-ray imaging technique as a combination of two distinct energies (low and high) has been introduced [1,2]. Motion artifacts occur because DE images are acquired through two exposures. To minimize these motion artifact problems due to patient motion, respiration and heart rate, a single shot DE technique using a sandwich-like multilayer detector was proposed [3]. By inserting intermediate filter between the two detector layers, the sandwich detector can produce low- and high-energy separated images, thereby resulting in higher contrast in the single-shot DE images [4,5,6].

However, the single-shot DE technique is less effective in the separation of two energies than the conventional DE technique and can further increase image noise. Because the single-shot DE technique is made with the two images separated by the intermediate filter that absorbs the low energy photons while transmitting the higher energy photons. Therefore, the design of the energy separation filter should be performed first for the successful single-shot DE x-ray imaging technique (i.e., optimal material and thickness) [7].

In this study, we investigate an optimal filter material and thickness that can give rise to the best signal-to-noise performance.

### 2. Theoretical background

#### 2.1 Sandwich detector

In previous study, the sandwich detector was theoretically modeled using cascaded-systems model (CSA) [8,9], and the performance of the sandwich detector for various kVp and intermediate filter thickness was analyzed [5,6]. The sandwich detector consisted of phosphor screens with different thickness: thinner for the front and thicker for the rear detector layers, respectively and intermediate filter for various materials and thickness. Therefore, the x-ray transmitted through the front detector and the intermediate filter reaches the rear detector, and the image corresponding to the relatively higher energy can be obtained the rear detector.

#### 2.2 Numerical phantom

A numerical phantom was used to mimic a mouse for the optimization calculations as illustrated in Fig. 1,

consisting of four polyurethane (PU,  $0.59 \text{ g cm}^{-3}$ ) disks with a thickness of 3 mm and an Al ( $2.7 \text{ g cm}^{-3}$ ) bar with a thickness of 1 mm embedded in 30 mm of polymethyl methacrylate (PMMA,  $1.18 \text{ g cm}^{-3}$ ). The disks and bar mimicked soft tissue and bone, respectively. This phantom was calculated from the attenuation coefficient for the 3% contrast of PU.

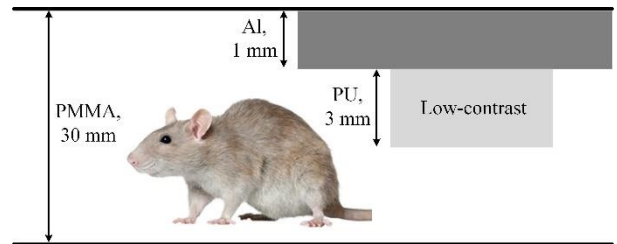


Figure 1. Numerical low-contrast phantom used to mimic a mouse.

#### 2.3 Dual-energy image signal, noise

A CSA model was previously introduced to address the signal and noise propagation in a sandwich detector and it is expanded in this study to include an expanded investigation of performance of each detector layer with respect to the applied kVp, the material and thickness of energy separation filter. For the average number of incident x-ray photon  $\bar{q}$  (quanta  $\text{mm}^{-2}$ ) at the entrance surface of the sandwich detector, the CSA model gives the average signal at the output of the  $j$ -th detector layer ( $F$  and  $R$  denotes the front and rear detector, respectively):

$$\bar{d}_j = ka^2 \bar{q} \bar{r}_j \bar{g}_j \quad (1)$$

The variance of signal measured from each detector layer can be calculated by the quadrature sum of each noise component:

$$\sigma_{j,total}^2 = \sigma_{j,indirect}^2 + \sigma_{j,direct}^2 + \sigma_{j,add}^2 \quad (2)$$

The relative variance due to indirect interaction can be estimated from the presampling NPS.

For the reconstruction of single-shot DE images, we apply the weighted log-subtraction method to the low- and high-energy images [11]:

$$I_{DE}(x, y) = I_R(x, y) - w I_F(x, y) \quad (3)$$

where,  $w$  is the weight for cancellation of uninterested objects.

As a figure of merit (FOM) for filter optimization, we combine the measured signal difference (SD) and noise ( $\sigma$ ) that is calculated from the CSA simulations:

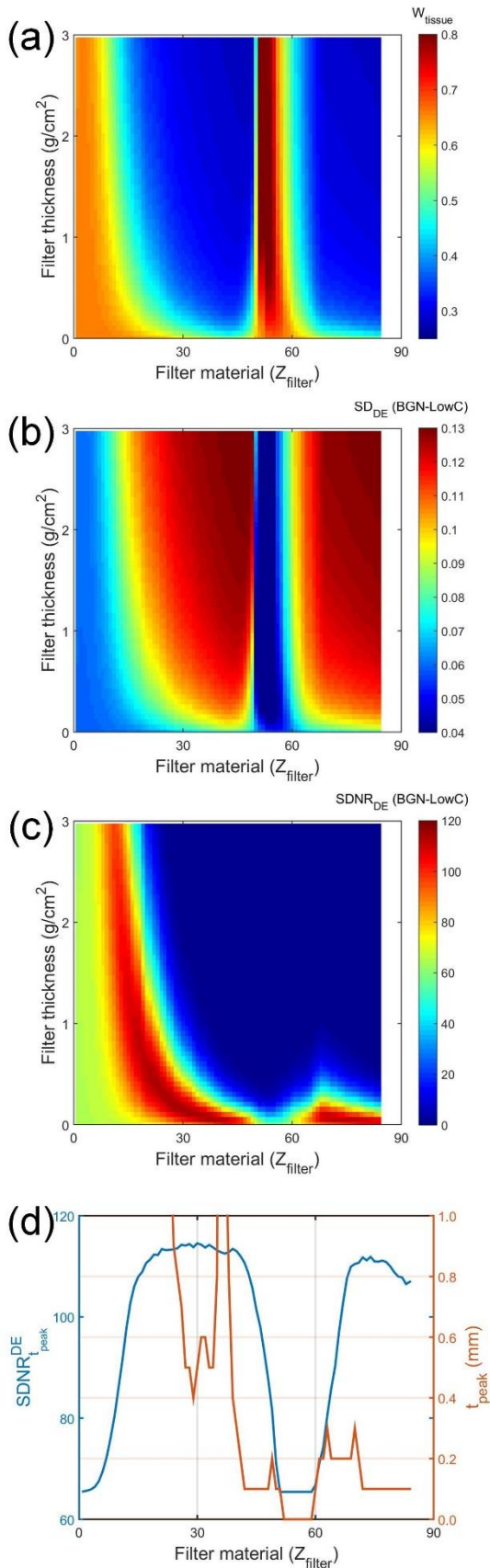


Figure 2 Effect of energy separation filter in dual-energy image performance. (a) tissue weighting parameter,  $w_s$ , (b) dual-energy signal difference, (c) dual-energy image signal-

difference to noise ratio,  $SDNR^{DE}$ , (d) Peak  $SDNR^{DE}$  and required filter thickness as a function of filter materials

$$FOM = \frac{SD_{DE}}{\sigma_{DE}} \quad (4)$$

### 3. Preliminary results

The DE imaging performance metrics on energy separation filter is shown in Fig. 2. Calculations are shown as a function of filter material type ( $Z_{filter}$ ) and thickness ( $s_{filter}$ ), with the single-exposure at 60 kVp. Figure 2(a) shows the reduction in tissue weighting parameter,  $w_s$ . The effect of energy separation on  $SD^{DE}$  is similar, as shown in Fig. 2(b). The higher atomic number increases the spectral separation and increase the DE signal difference at  $Z_{filter}$ . While a higher atomic number increase PU contrast, the trade-off in image noise and  $SDNR^{DE}$  is showed in Fig. 2(c). The peak  $SDNR^{DE}$  from Fig. 2(c) and the associated filter thickness are shown in Fig. 3(d).

### 4. Further study

The remained further study before the meeting includes the followings:

- DE  $SDNR$  calculation based on low contrast percentage (i.e., 1 ~ 5 % contrast) using the CSA model;
- Calculation of x-ray Swank factor by filter materials, thickness and x-ray energy;
- Optimum energy separation filter material and thickness extraction form the highest DE  $SDNR$ ;

### Acknowledgments

This work was supported by the National Research Foundation of Korea (NRF) grant funded by the Korean government (MSIP) (No. 2017M2A2A6A01019930).

### REFERENCES

- [1] R. E. Alvarez, J. A. Seibert, and S. K. Thompson, Comparison of dual energy detector system performance, *Med. Phys.*, Vol. 31, No. 3, pp. 556-565, 2004.
- [2] S. Richard and J. H. Siewerdsen, Optimization of dual-energy imaging systems using generalized NEQ and imaging task, *Med. Phys.*, Vol. 34, No. 1, pp. 127-139, 2007
- [3] S. Yun, J. C. Han, D. W. Kim, H. Youn, H. K. Kim, J. Tanguay, and I. A. Cunningham, Feasibility of active sandwich detectors for single-shot dual-energy imaging, *Proc. SPIE 9033*, p. 90335T, 2014.
- [4] D. W. Kim, H. K. Kim, H. Youn, S. Yun, J. C. Han, J. Kim, S. Kam, J. Tanguay, and I. A. Cunningham, Signal and noise analysis of flat-panel sandwich detectors for single-shot dual-energy x-ray imaging, *Proc. SPIE 9413*, p. 94124A-1, 2015.
- [5] D. W. Kim, J. Kim, S. Yun, H. Youn, and H. K. Kim, Cascaded-systems analysis of sandwich x-ray detectors, *J. Instrum.*, Vol. 11, No. 12, p. C12022, 2016
- [6] J. Kim, D. Kim, S. Kam, E. Park, H. Youn, and H. K. Kim, Effects of the energy-separation filter on the performance of each detector layer in the sandwich detector for single-shot dual-energy imaging, *J. Instrum.*, Vol.11, No.2, pp. C02065,

2016.

[7] N. A. Shkumat, J. H. Siewerdsen, A. C. Dhanantwari, D. B. Williams, N. S. Paul, J. Yorkston, R. Van Metter, Optimization of image acquisition techniques for dual-energy imaging of the chest, *Med. Phys.*, Vol.3, No.10, pp. 3904–3915, 2007

[8] I. A. Cunningham, M. S. Westmore, and A. Fenster, A spatial-frequency dependent quantum accounting diagram and detective quantum efficiency model of signal and noise propagation in cascaded imaging systems, *Med. Phys.*, Vol 21, No. 3, pp. 417-427, 1994.

[9] J. H. Siewerdsen, L. E. Antonuk, Y. El-Mohri, J. Yorkston, W. Huang, J. M. Boudry, and I. A. Cunningham, Empirical and theoretical investigation of the noise performance of indirect detection, active matrix flat-panel imagers (AMFPIs) for diagnostic radiology, *Med. Phys.*, Vol. 24, No. 1, pp. 71-89, 1997.

[10] A. R. N. 31, Standardized methods for measuring diagnostic x-ray exposure, tech. rep., American Association of Physicists in Medicine, 1990.

[11] J. M. Sbol, G.B. Avinash, F. Nicolas, B. Claus, J. Zhao, and J. T. Dobbins, The development and characterization of a dual-energy subtraction imaging system for chest radiography based on CsI:Tl amorphous silicon flat-panel technology, in *Proc. SPIE*, vol. 4320, pp. 3990408, 2001.